

# Momentum Transfer Dependence of Inelastic X-Ray Scattering from the Li *K* Edge

M. H. Krisch, F. Sette, C. Masciovecchio, and R. Verbeni

*European Synchrotron Radiation Facility, B.P. 220, F-38043 Grenoble Cedex, France*

(Received 16 October 1996)

Inelastic x-ray scattering from the *K* edge of lithium metal at 30 K is measured at momentum transfers  $q = 8.8$  and  $97.3 \text{ nm}^{-1}$  with 80 meV energy resolution. The transition from dipolar ( $1s \rightarrow p$ ,  $q = 8.8 \text{ nm}^{-1}$ ) to monopolar ( $1s \rightarrow s$ ,  $q = 97.3 \text{ nm}^{-1}$ ) excitations is demonstrated by differences in the spectra reflecting either the *p* or *s* partial density of states above the Li Fermi level. The Mahan-Nozières-De Dominicis theory is utilized to determine *both* threshold exponents  $\alpha_0$  and  $\alpha_1$  from the present *K*-edge data. [S0031-9007(97)02892-5]

PACS numbers: 78.70.Dm, 71.45.Gm, 78.70.Ck

The relevance of many-body effects in the x-ray absorption and emission spectra of simple metals has been widely discussed since the pioneering work of Mahan, Nozières, and De Dominicis [1,2] (MND), and up to more refined recent theories [3–5]. The screening of the core-hole potential by the conduction electrons with energies close to the Fermi level induces anomalies in the absorption and emission thresholds, which can be described in the near-threshold region by a power law. In its simplest formulation [1,2], the spectral shape  $I(\hbar\omega)$  near an x-ray threshold  $\hbar\omega_0$  can be expressed as follows:

$$I(\hbar\omega) \propto \sum_{l=0}^{\infty} |W_l(\hbar\omega)|^2 \left( \frac{\xi}{\hbar(\omega - \omega_0)} \right)^{\alpha_l}, \quad (1)$$

where  $\xi$  is a range parameter of the order of the kinetic energy of the electrons at the Fermi level, and  $|W_l|^2$  is proportional to the transition density of states (TDOS) between the core level and the conduction electron states with angular quantum number *l*. The many-body effect, arising from the screening of the core hole by the valence electrons, is contained in the threshold exponents  $\alpha_l$ . The threshold intensity is enhanced or reduced with respect to the one-electron TDOS depending upon the sign and the magnitude of  $\alpha_l$ . These exponents are proportional to the phase shifts,  $\delta_l$ , describing the scattering of the conduction electrons from the core-hole, and are expected to be related among each other and to the total singularity index,  $\alpha$ , by a series of sum rules [1,6]. Equation (1) is expected to be valid in the near-threshold region, typically within a fraction of the range parameter  $\xi$ .

The experimental observation of threshold anomalies is obscured by the core-hole lifetime, the experimental resolution, the shape of the density of states, and eventual additional broadening due to phonons. The importance of these effects has been well established in the  $L_{2,3}$  edges of Na, Mg, and Al [7,8], and has been reviewed by Citrin *et al.* [7], Mahan [8], and Ohtaka and Tanabe [9].

The case of the Li *K* edge is still partly unclear. Experimental values are available for  $\alpha$  and  $\alpha_1$ , but they are inconsistent among each other when the relations imposed by the sum rules are utilized [10]. Using  $\alpha_1 \approx 0$ , as determined from x-ray absorption measurements [7,11],  $\alpha$

is derived to be 0.17, and  $\alpha_0 = 0.33$ . Similarly, using  $\alpha = 0.23$ , as determined from the Li *1s* x-ray photoemission line shape [12], one obtains  $\alpha_1 = -0.11$  and  $\alpha_0 = 0.42$ . The inconsistencies among  $\alpha_1$  and  $\alpha$ , as well as the large positive value of  $\alpha_0$  (which should lead to a very peaked absorption threshold for  $1s \rightarrow s$  transitions), could be due to different factors: the utilized theoretical line shape may be too simplistic, and/or the sum rules may not be applicable because they neglect the possible dependence of the exponents on the exchange interaction among the core and the valence electrons [13]. The simple line shape expressed in Eq. (1) has the advantage of a reasonably easy comparison with the experimental data without too many parameters entering in the fit, and can be justified theoretically when limited to energy ranges comparable to the intrinsic threshold linewidth [7,9]. In summary, it appears that, in lithium, the only way to obtain convincing values of the threshold exponents is by their independent experimental determination. This is possible, in principle, using electron energy loss spectroscopy (EELS) [14] or inelastic x-ray scattering (IXS) [15] to determine the momentum transfer ( $\hbar q$ ) dependence of excitations from the considered core level to states just above the Fermi level. In fact, for  $1/q$  large with respect to the spatial extension  $r_0$  of the core-hole wave function, the interaction operator  $e^{i\vec{q}\cdot\vec{r}}$  can be approximated by  $\vec{q} \cdot \vec{r}$ . Then, the inelastic scattering is formally identical to x-ray absorption (emission) in the dipole approximation, and the direction of the wave vector  $\vec{q}$  plays the role of the polarization vector  $\vec{e}$  [16]. On the contrary, at large  $q$ , i.e., for  $q \geq q_0 = 1/r_0$ , all poles in the spherical harmonics expansion of  $e^{i\vec{q}\cdot\vec{r}}$  contribute to the spectrum, providing that there are final states with the appropriate symmetry to couple to the core wave function.

The  $q$ -dependent TDOS for the Li *K* edge ( $r_0 \approx 0.02 \text{ nm}$  and  $q_0 = 50 \text{ nm}^{-1}$ ), calculated by Doniach *et al.* [15], shows that, for  $qr \geq 1$ , the  $1s \rightarrow p$  and  $1s \rightarrow d$  excitations are suppressed and only the monopolar  $1s \rightarrow s$  transitions are left. Momentum dependent EELS data were taken with  $q$  values in the  $\approx 0$  to  $12 \text{ nm}^{-1}$  range [14]:  $\alpha_1 \approx 0$  was confirmed from the

small  $q$  data, while at the larger  $q$  values—still not large enough to suppress the dipolar contribution—no spectral modifications were detected that could be associated with a value of  $\alpha_0$  different from that of  $\alpha_1$ . Similarly, momentum dependent IXS measurements on lithium were performed up to  $q = 19 \text{ nm}^{-1}$  [17]. In this case, however, the energy resolution of 0.8 eV, large compared to the Li  $K$ -edge intrinsic width of  $\approx 300 \text{ meV}$ , limited the capability to pinpoint any  $q$  dependence in the  $K$ -edge shape. This scenario motivated the present inelastic x-ray scattering study.

In this Letter we report  $q$ -dependent high energy resolution inelastic x-ray measurements of the lithium metal  $K$  edge. Our results show the transition from dipolar  $1s \rightarrow p$  excitations at  $q = 8.8 \text{ nm}^{-1}$ , to monopolar  $1s \rightarrow s$  excitations at  $q = 97.3 \text{ nm}^{-1}$ . The observed  $q$  dependence of the IXS spectra is consistent with the calculated partial  $p$  and  $s$  densities of states in lithium. The analysis of the near-edge spectral shape at these two  $q$  values, which are either well below or above  $q_0$ , allows the independent experimental determination of the threshold exponents  $\alpha_0$  and  $\alpha_1$ . We obtain a negative value for  $\alpha_0$ , which is inconsistent with the positive one predicted by the sum rules, while the value of  $\alpha_1$  confirms previous results. Our values of  $\alpha_0$  and  $\alpha_1$  are, however, in very good agreement with those calculated by Girvin and Hopfield taking into account exchange effects [13]. Therefore, our results strongly support their view that the exchange interaction among the core hole and the conduction electrons is important in the screening of the core-hole potential, and that this process contributes to the determination of the observed shape of the  $K$ -edge threshold in lithium. More generally, this work demonstrates that IXS from low  $Z$  element core levels can now be performed with an energy resolution comparable to EELS in an extended  $q$  range.

The experiment was performed on the inelastic x-ray scattering beam line BL21-ID16 at the European Synchrotron Radiation Facility. Undulator radiation was monochromatized by a cryogenically cooled Si(111) double crystal, followed by a Si(444) dispersive four-crystal device [Si(444) nondispersive two-crystal device], and the measured resolution function could be well approximated by a Gaussian of 40 (210) meV full-width-half-maximum (FWHM) at  $\approx 10 \text{ keV}$  x-ray energies. The incident flux on the sample was typically  $1 (5) \times 10^{11}$  photons/s. The scattered radiation was analyzed in the horizontal plane by a Rowland circle crystal spectrometer with a radius of 1 m, operating at a fixed energy of 9885 eV. The overall experimental resolution was either 80 or 210 meV in the two monochromator configurations as determined from elastic scattering measurements [18]. The sample was a polycrystalline lithium metal rod of 12 mm diameter (Goodfellow) kept in vacuum at 30 K. Spectra were recorded at scattering angles of  $10^\circ$  and  $150^\circ$ , corresponding to momentum transfers  $8.8$  and  $97.3 \text{ nm}^{-1}$ , and to  $qr$  values of 0.174 and 1.93, respectively. There-

fore, in the  $K$ -edge threshold region, on the basis of the results of Ref. [15], the spectrum at  $q = 8.8 \text{ nm}^{-1}$  should be dominated by  $1s \rightarrow p$  dipolar excitations as in photoabsorption, while at  $q = 97.3 \text{ nm}^{-1}$ , only the  $1s \rightarrow s$  monopolar excitations should contribute.

The top of Figs. 1(a) and 1(b) reports the spectra at  $q = 8.8 \text{ nm}^{-1}$  [Fig. 1(a)] and  $q = 97.3 \text{ nm}^{-1}$  [Fig. 1(b)] as a function of the energy transfer  $\hbar\omega$ , which is the difference between incident ( $\hbar\omega_1$ ) and scattered ( $\hbar\omega_2$ ) photon energies, minus the Li  $K$ -edge threshold energy,

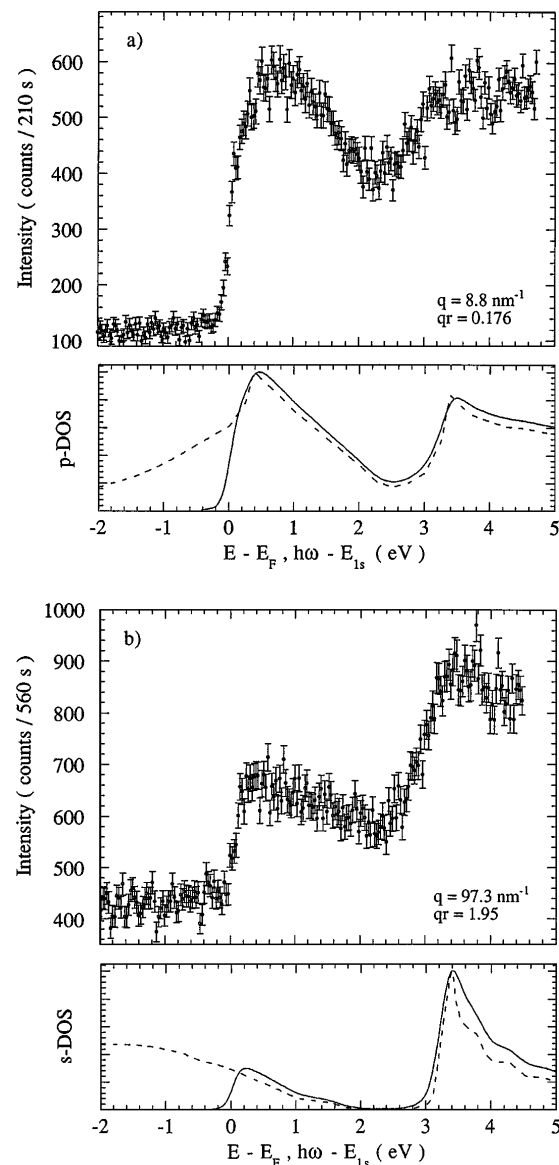


FIG. 1. Inelastic x-ray scattering spectra from the Li  $K$  edge at momentum transfers  $q = 8.8 \text{ nm}^{-1}$  (a) and  $97.3 \text{ nm}^{-1}$  (b) as a function of energy transfer,  $\hbar\omega$ , minus the Li  $K$ -edge absorption threshold value  $E_{1s} = 54.9 \text{ eV}$ . This energy scale corresponds also to that of the one-electron energies  $E$  referred to the Fermi energy  $E_F$  ( $E - E_F$ ). The data are shown with their error bars. The bottom panels show the  $p$  (a) and  $s$  (b) partial densities of states (dashed lines), and its empty part above the Fermi level convoluted with the broadening functions as described in the text (solid line).

$E_{1s} = 54.9$  eV [11]. In the one-electron picture, this energy scale corresponds also to the electron energy  $E$  referred to the Fermi energy  $E_F$ . In the spectrum at  $q = 8.8$  nm $^{-1}$ , the half-height position of the edge is located at 54.9 eV, and the width corresponding to 10% to 90% intensity is 400 meV. The change in slope, best visible in the upper part of the edge, is consistent with previous observations [11]. The edge is followed by two broad features of comparable intensity at  $\approx 0.5$  and 3.4 eV, separated by a minimum at about 2.5 eV. In the spectrum at momentum transfer  $q = 97.3$  nm $^{-1}$ , shown in Fig. 1(b), there are few clear spectral differences. In particular, (i) the edge width is reduced to 240 meV, (ii) the change of slope in the upper part of the edge is no longer visible, and (iii) the two features have changed their relative weight, with the second one increasing in intensity by approximately a factor of 2.

The bottom panels of Figs. 1(a) and 1(b) report calculated  $p$  and  $s$  partial densities of states (DOS) (dashed lines) [19]. The empty part of these partial DOS have been convoluted with a 40 meV FWHM Lorentzian curve, representing the Li 1s core-hole lifetime [7], and two Gaussian curves of 200 and 80 meV FWHM, representing, respectively, the phonon broadening [20] and the instrumental resolution (solid line). The consistency between experiment and convoluted partial empty DOS is apparent. The 400 meV edge width at  $q = 8.8$  nm $^{-1}$  is explained by the rising  $p$  DOS at the Fermi level, leading to a change of slope at the edge [11]. Similarly, the edge-width reduction at  $q = 97.3$  nm $^{-1}$  is a consequence of the  $s$  DOS, which is monotonically decreasing around the Fermi level. Moreover, the energy position of the first two features above the edge, as well as their relative intensity, are in good agreement with the experimental spectra. These observations demonstrate that the observed  $q$  dependence in the core absorption spectra is due to different selection rules, namely, the dipolar  $1s \rightarrow p$  channel at  $q = 8.8$  nm $^{-1}$ , and the monopolar  $1s \rightarrow s$  channel at  $q = 97.3$  nm $^{-1}$ . Our results sensibly extend the  $q$  range covered by the previous EELS measurements [14], where no  $q$  dependence of the edge shape was found for momentum transfers up to 12 nm $^{-1}$ .

The relevance of many-body effects on the shape of the Li  $K$  edge, and its  $q$  dependence, cannot be reliably determined from the data shown in Fig. 1 as a consequence of their statistical accuracy. An increase by a factor of 5 in the incident photon flux was obtained by removing the second crystal pair of the dispersive monochromator. This induces an increase of the total energy resolution to  $\approx 210$  meV [18], a value still comparable to the intrinsic width of the Li  $K$ -edge threshold.

The experimental data up to 0.4 eV above threshold, taken at  $q = 8.8$  and 97.3 nm $^{-1}$ , are reported in Figs. 2(a) and 2(b), together with the corresponding fits and error analysis to be discussed in the following. In this region, it is reasonable to neglect the energy dependence of the transition matrix element and of the

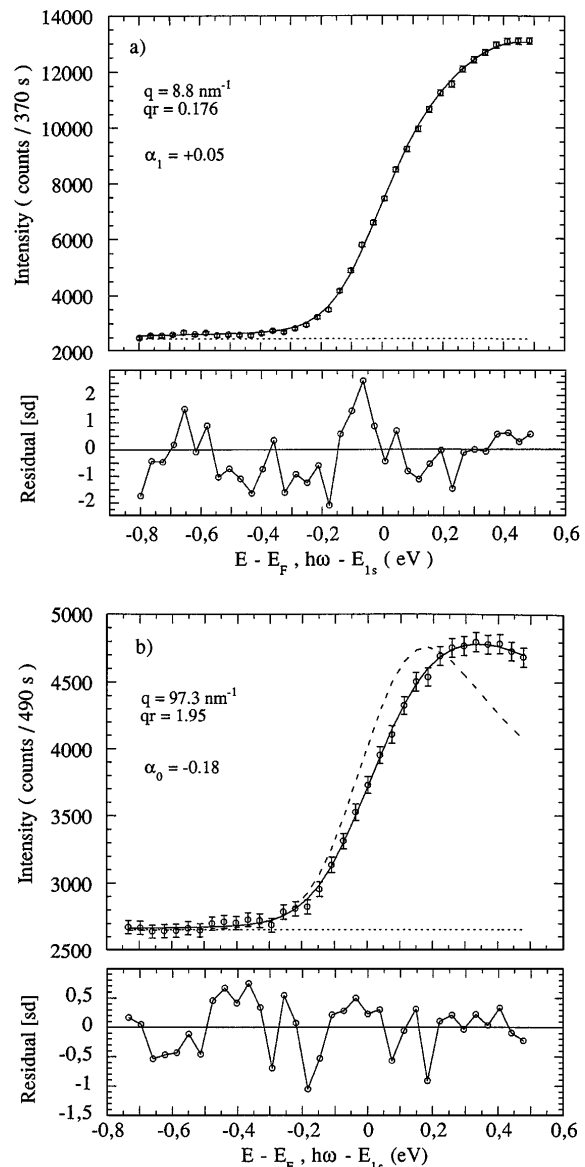


FIG. 2. Inelastic x-ray scattering spectra in the immediate vicinity of the Li  $K$  edge at  $q = 8.8$  nm $^{-1}$  (a) and 97.3 nm $^{-1}$  (b). The data ( $\circ$ ), shown with their error bars, are superimposed to the fit (solid line) obtained as explained in the text. The dotted line corresponds to the background whose slope has been determined from the data below the edge. The bottom panels report the difference between the data and the fit for each data point in standard deviation units (sd). The dashed line in the top panel of (b) has been obtained keeping constant in the fit the values of  $\alpha_0$  and of the Gaussian broadening, respectively, to 0.274 and 290 meV FWHM.

threshold exponents [9]. The fitting function, therefore, has been modeled by the product of the partial empty densities of states shown in Fig. 1 ( $p$  DOS at  $q = 8.8$  nm $^{-1}$  and  $s$  DOS at  $q = 97.3$  nm $^{-1}$ ) times the energy dependent term  $[1/\hbar(\omega - \omega_0)]^{\alpha_l}$ . The broadening is introduced by the convolution of this model function with a Lorentzian of 40 meV FWHM representing the lifetime broadening [7], and with a Gaussian of adjustable width, expected to be  $\approx 300$  meV

FWHM, accounting for the phonon broadening ( $\approx 200$  meV [20]) and the instrumental resolution function (210 meV). The background was determined by a linear fit of the data in the pre-edge region ( $\hbar\omega$ : 51 to 53.5 eV), and the slope was kept constant in the fit of the edge shape [21]. The background corresponds to the dotted lines in Fig. 2. The fits to the experimental curves were performed using standard  $\chi^2$  minimization. A constant background, the Gaussian width, the intensity (including the range parameter  $\xi$ ), and the threshold exponent  $\alpha_l$  were left as free parameters. In the bottom panels of Figs. 2(a) and 2(b), we show the difference between the data and the fitting function in units of 1 standard deviation (sd) for each data point. The best fit gives  $\alpha_0 = -0.18 \pm 0.07$  and  $\alpha_1 = 0.05 \pm 0.03$ . The uncertainties were determined from the parameter's values corresponding to either an increase by a factor of 2 of the  $\chi^2$ , or when the fit yielded unacceptable values for the width of the resolution function. The best value for the Gaussian broadening was 290 meV FWHM in both spectra, consistent with our energy resolution and the expected phonon broadening.

The value of  $\alpha_1$  is comparable with those determined by soft x-ray absorption and EELS measurements. The  $\alpha_0$  value, however, is in disagreement with the prediction that transitions to final states of  $s$  symmetry should give a large positive  $\alpha_0$  ( $\alpha_0 \approx 0.33$  or  $\approx 0.42$  using the sum rules and the previous experimental values of either  $\alpha_1$  or  $\alpha$ ). The size of this inconsistency is emphasized by the comparison among the experimental spectrum, the best fit, and the dashed line in the top panel of Fig. 2(b), which is obtained repeating the fit with  $\alpha_0$  fixed to 0.274 (derived using our  $\alpha_1$  and the sum rules) and the Gaussian width to 290 meV FWHM.

In contrast, our values of  $\alpha_0$  and  $\alpha_1$  are in very good agreement with those derived by Girvin and Hopfield [13], who included exchange in the calculation of the phase shifts  $\delta_l$ . They obtain  $\alpha_0 = -0.164$  and  $\alpha_1 = +0.044$ . The present independent determination of  $\alpha_0$  and  $\alpha_1$  confirms, therefore, the relevance of magnetic interactions in the screening of the lithium  $1s$  core hole. These exchange effects, well known for localized electronic states and well understood whenever one can utilize an atomic picture, have always been a challenge in almost free-electron-like systems as lithium. The possibility to access them experimentally renews important challenges to the theory, and may provide a framework to get information on spin-dependent electron-electron correlation functions.

In summary, we have shown that different final state symmetries of an excited core electron can be probed by varying the momentum transfer in an inelastic x-ray scattering experiment. In the specific case of lithium metal, the transition from dipolar to monopolar transitions

is convincingly demonstrated by the comparison of the  $q$ -dependent spectral shapes with the partial empty density of states above the Fermi level. The data analysis underlines the importance of exchange effects in the description of the  $K$  edge in lithium.

We acknowledge valuable discussions with M. Altarelli, and the technical assistance by B. Gorges and J.-F. Ribois.

- 
- [1] G. D. Mahan, Phys. Rev. **163**, 612 (1967).
  - [2] P. Nozières and C. T. De Dominicis, Phys. Rev. **178**, 1097 (1969).
  - [3] K. Ishikawa, Y. Ohmura, and Y. Mizuno, J. Phys. Soc. Jpn. **34**, 324 (1973).
  - [4] Y. Ohmura, K. Ishikawa, and Y. Mizuno, J. Phys. Soc. Jpn. **36**, 370 (1974).
  - [5] Y. Ohmura and K. Ishikawa, J. Phys. Soc. Jpn. **49**, 1829 (1980).
  - [6] J. Friedel, Philos. Mag. **43**, 153 (1952).
  - [7] P. H. Citrin, G. K. Wertheim, and M. Schlüter, Phys. Rev. B **20**, 3067 (1979).
  - [8] G. D. Mahan, in *Fermi Surface Effects*, edited by J. Kondo and A. Yoshimori (Springer, Berlin, 1988), p. 41ff.
  - [9] K. Ohtaka and Y. Tanabe, Rev. Mod. Phys. **62**, 929 (1990).
  - [10] J. D. Dow, Phys. Rev. Lett. **31**, 1132 (1973). This derivation is done assuming that  $\delta_l = 0$  for  $l \geq 2$ .
  - [11] H. Petersen, Phys. Rev. Lett. **35**, 1363 (1975).
  - [12] P. H. Citrin, G. K. Wertheim, and Y. Baer, Phys. Rev. B **16**, 4256 (1977).
  - [13] S. M. Girvin and J. J. Hopfield, Phys. Rev. Lett. **37**, 1091 (1976).
  - [14] J. J. Ritsko, S. E. Schnatterly, and P. C. Gibbons, Phys. Rev. B **10**, 5017 (1974).
  - [15] S. Doniach, P. M. Platzman, and J. T. Yue, Phys. Rev. B **4**, 3345 (1971).
  - [16] Y. Mizuno and Y. Ohmura, J. Phys. Soc. Jpn. **22**, 445 (1967).
  - [17] H. Nagasawa, S. Mourikis, and W. Schülke, J. Phys. Soc. Jpn. **58**, 710 (1989).
  - [18] The experimental resolution function in the 210 meV monochromator configuration is almost completely determined by the monochromator. In the 40 meV monochromator configuration, we measure a total width of 80 meV and a shape still well represented by a Gaussian from the elastic scattering of a plastic amorphous sample.
  - [19] D. A. Papaconstantopoulos, in *Handbook of the Band Structure of Elemental Solids* (Plenum Press, New York and London, 1986).
  - [20] Y. Baer, P. H. Citrin, and G. K. Wertheim, Phys. Rev. Lett. **37**, 49 (1976).
  - [21] The major source for the background slope is due to the tails of valence excitations at small  $q$ , and from the Compton profile at large  $q$ . These contributions were determined from wide energy scans, and they can be well approximated by a linear background in the small energy region considered here.